RNA (2000), *6*:1289–1305. Cambridge University Press. Printed in the USA.

The carboxy terminal WD domain of the pre-mRNA splicing factor Prp17p is critical for function

LAURA A. LINDSEY-BOLTZ,[1]* GEETANJALI CHAWLA,[2]* N. SRINIVASAN,[3] USHA VIJAYRAGHAVAN,[2] and MARIANO A. GARCIA-BLANCO[1,4]

[1]Program in Molecular Cancer Biology, Duke University Medical Center, Durham, North Carolina 27710, USA
[2]Department of Microbiology and Cell Biology, Indian Institute of Science, Bangalore: 560 012, India
[3]Molecular Biophysics Unit, Indian Institute of Science, Bangalore: 560 012, India
[4]Department of Genetics, Microbiology, and Medicine, Duke University Medical Center, Durham, North Carolina 27710, USA

ABSTRACT

In *Saccharomyces cerevisiae*, Prp17p is required for the efficient completion of the second step of pre-mRNA splicing. The function and interacting factors for this protein have not been elucidated. We have performed a mutational analysis of yPrp17p to identify protein domains critical for function. A series of deletions were made throughout the region spanning the N-terminal 158 amino acids of the protein, which do not contain any identified structural motifs. The C-terminal portion (amino acids 160–455) contains a WD domain containing seven WD repeats. We determined that a minimal functional Prp17p consists of the WD domain and 40 amino acids N-terminal to it. We generated a three-dimensional model of the WD repeats in Prp17p based on the crystal structure of the β-transducin WD domain. This model was used to identify potentially important amino acids for in vivo functional characterization. Through analysis of mutations in four different loops of Prp17p that lie between β strands in the WD repeats, we have identified four amino acids, $_{235}$TETG$_{238}$, that are critical for function. These amino acids are predicted to be surface exposed and may be involved in interactions that are important for splicing. Temperature-sensitive *prp17* alleles with mutations of these four amino acids are defective for the second step of splicing and are synthetically lethal with a U5 snRNA loop I mutation, which is also required for the second step of splicing. These data reinforce the functional significance of this region within the WD domain of Prp17p in the second step of splicing.

Keywords: β propeller; homology modeling; mutational analysis; nuclear localization; Prp17; second-step splicing; U5 snRNA

INTRODUCTION

Precursors of messenger RNAs (pre-mRNAs) of many eukaryotic genes contain intervening sequences (introns) that are removed during maturation of the mRNA by a process called pre-mRNA splicing. The precise removal of introns is an important event in gene expression and provides a level of posttranscriptional regulation. Pre-mRNA introns are removed via a two-step mechanism. In the first step the 5′ exon is cleaved concomitant with the production of a lariat intermediate. In the second step the exons are joined, and the intron is released in the form of a lariat product. A large enzyme called the spliceosome, which consists of five small nuclear RNAs (snRNAs) and at least 70 proteins, identifies the splice sites and then catalyzes the two reactions. The reaction mechanism and many of the components of the spliceosome are conserved from yeast to humans (Burge et al., 1999).

Genetic studies in the budding yeast *Saccharomyces cerevisiae* have identified four gene products (Prp16p, Prp17p, Prp18p, and Slu7p) required exclusively for the second step of pre-mRNA splicing (Couto et al., 1987; Vijayraghavan et al., 1989; Frank et al., 1992; reviewed in Umen & Guthrie, 1995c). Subsequently, human homologs of these genes have been cloned based on sequence similarity and their role in the second step of human pre-mRNA splicing reported (Horowitz & Krainer, 1997; Ben Yehuda et al., 1998; Lindsey & Garcia-Blanco, 1998; Zhou & Reed, 1998; Chua & Reed, 1999). The precise functions of these second-step proteins in both yeast

Reprint requests to: Mariano A. Garcia-Blanco, Department of Genetics, 424 CARL, Duke University Medical Center, Durham, North Carolina 27710, USA; e-mail: garci001@mc.duke.edu; or Usha Vijayraghavan, Department of Microbiology and Cell Biology, Indian Institute of Science, Bangalore: 560 012, India; e-mail: uvr@mcbl.iisc.ernet.in.
*These authors are joint first authors.

and humans are only now being unraveled. Unique genetic interactions between these four factors in yeast have led to the suggestion that they associate physically or functionally with each other (Frank et al., 1992; Jones et al., 1995; Seshadri et al., 1996). Among these factors, the function of Prp17p, which is nonessential in yeast, is not well characterized.

In yeast, the second-step factors have been ordered with respect to an ATP-dependent event during the second step (Schwer & Guthrie, 1991; Horowitz & Abelson, 1993; Ansari & Schwer, 1995; Jones et al., 1995). The RNA helicase Prp16p hydrolyzes ATP and is required for a conformational change that occurs in the spliceosome after the first step (Schwer & Guthrie, 1992). yPrp17p is required before or during this event; Prp18p and Slu7p are required afterwards (Umen & Guthrie, 1995b). A role for the yeast Prp22 in the second step of splicing has been shown more recently (Schwer & Gross, 1998), and it is proposed to act in conjunction with Slu7 and Prp18. Rearrangements in the spliceosome after the first step are required to identify and position the 3′ splice site for the second step. After the first step of splicing, the highly conserved loop I of U5 snRNA plays an important role in aligning the two exons for the second-step catalytic site. In yeast, this loop is essential for the second step; however, in humans it is not required (O'Keefe et al., 1996; Segault et al., 1999). The loop I uridines are likely involved in noncanonical base pairing with the exon sequences near the splice sites, which are weakly conserved compared to elements in the intron. Additional interactions appear to be necessary for stabilization of the U5 snRNA and the two exons during the second step. For example, the highly conserved U5 snRNP protein Prp8p crosslinks to both the 5′ and 3′ splice sites (Wyatt et al., 1992; Teigelkamp et al., 1995; Umen & Guthrie, 1995a, 1995b). In addition, Slu7p and yPrp17p have been linked genetically to the function of U5 snRNA loop I (Frank et al., 1992; Seshadri et al., 1996).

Prp18p and Slu7p have been shown to physically interact (Zhang & Schwer, 1997); however, no other direct interactions have been shown between proteins required for the second step. Studies of synthetic lethality suggest that there is a functional interaction between all the second-step factors (reviewed in Umen & Guthrie, 1995c). Alleles of *PRP17* are synthetically lethal with alleles of *SLU7*, *PRP16*, *PRP18*, *PRP8*, *SLT11*, U5 snRNA, and U2 snRNA (Frank et al., 1992; Umen & Guthrie, 1995a; Seshadri et al., 1996; Xu et al., 1998), implying specific, and possibly direct interactions. Insufficient knowledge of the proteins and/or RNAs that interact with yPrp17p, and the function of this protein, severely limits our understanding of its role in the second step of pre-mRNA splicing. Through computer modeling of a conserved domain in yPrp17 protein and mutational analysis of this protein we have uncovered essential domains in this factor.

The most highly conserved region between the yeast and human Prp17 proteins is the C-terminal domain, where both contain seven WD repeats (Fig. 1A). The sequence similarity in this domain also extends to the Prp17 homologs in *Caenorhabditis elegans* and *Schizosaccharomyces pombe* (Ben Yehuda et al., 1998; Lindsey & Garcia-Blanco, 1998). WD repeats, also known as WD-40 repeats, consist of approximately 40 amino acids characterized by a conserved core of amino acids usually bound by glycine-histidine (GH) and tryptophan-aspartic acid (WD) (Fig. 2A). These proteins have a wide variety of cellular functions, and many are involved in coordinating protein–protein interactions in large multiprotein complexes (Neer et al., 1994; Neer & Smith, 1996). The prototypical members of this family are the β subunits of heterotrimeric G proteins. The crystal structure of β transducin has been solved (Wall et al., 1995; Lambright et al., 1996; Sondek et al., 1996), and it is likely that all members of the WD-repeat superfamily will fold into a similar seven-blade β propeller structure (Neer & Smith, 1996).

We generated a theoretical structure for the conserved WD motifs in Prp17 protein and then utilized phylogenetic conservation to identify potentially critical amino acids for function. Our computer model of the three-dimensional structure of the WD domain in yPrp17p took into consideration the three-dimensional structural features of Gβ and relationships at each residue position. Predicted solvent-exposed yet phylogenetically conserved residues were targeted for mutational analysis to identify critical residues in the WD domain. We also introduced a series of deletions in the N-terminal region of the protein that is outside of the WD domain to define their contribution to function. We found that a truncated yPrp17p consisting of only the WD domain and 40 amino acids N-terminal to it was fully functional under the conditions tested. In addition, we have identified four specific amino acids within the WD domain necessary to rescue the null phenotype and required for the second step of splicing. These four amino acids, $_{235}$TETG$_{238}$, are predicted to reside on the surface of the protein, and are probably a site for protein–protein interactions. Our modeling of two different mutations of these amino acids suggest that structural perturbations in this region underlie the temperature-sensitive nature of these mutants. We have also shown that mutations of these four amino acids are synthetically lethal with a specific mutation (*U98A*) in loop I of U5 snRNA. Therefore, these four amino acids in the WD domain may be involved in an interaction that becomes essential when U5 snRNA is mutated. In addition, we have defined amino acids 42–61 as those required for nuclear localization of protein. The results from these studies provide insight into the Prp17 protein and its interacting partners that influence 3′ splice site selection during the second step of splicing.

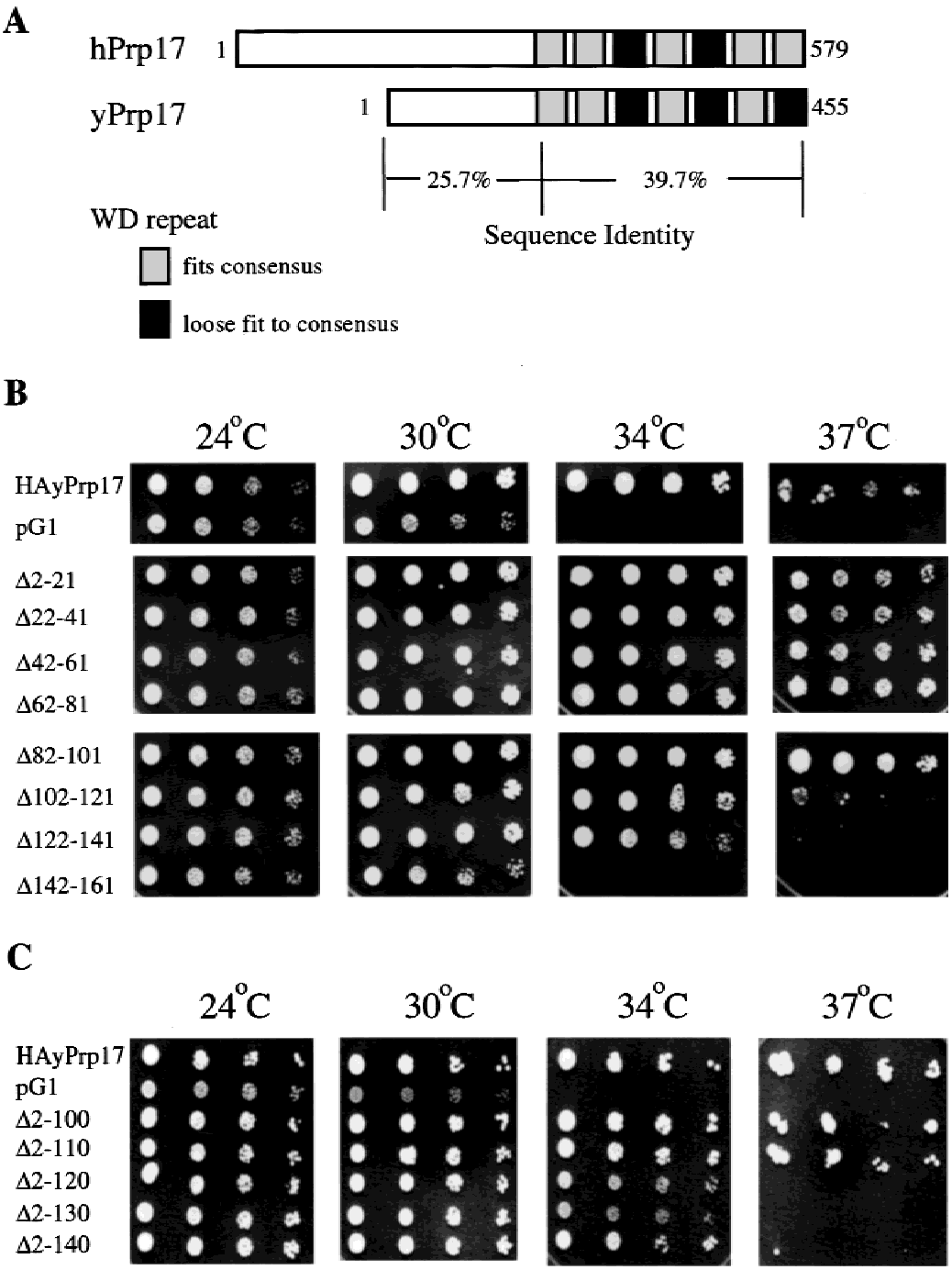

FIGURE 1. Deletion analysis of the N-terminal of yPrp17p. **A**: Comparison of hPrp17 and yPrp17p. The C-terminal end of these proteins, with 39.7% identity, is more highly conserved than the N-terminus, which has 25.7% identity. The positions of the WD repeats, as defined by Neer and Smith (1996), within each protein are boxed. The dark shaded boxes represent the WD repeats with a relatively poor match to the consensus, and the ones previously undefined in the yeast protein. **B**,**C**: The Δprp17 yeast strain was transformed with the wild-type HAyPRP17, the pG1 vector alone, or with pG1 containing the mutated *PRP17* sequences. Fivefold serial dilutions were made of the yeast, which were then grown on medium lacking tryptophan at 25 °C, 30 °C, 34 °C, or 37 °C.

RESULTS

Deletion analysis of the N-terminal domain reveals a 40-amino-acid essential domain

The region spanned by the N-terminal 158 amino acids of yPrp17p contains no recognizable motifs and is not highly conserved between yeast and humans (25.7% identity, Fig. 1A). To ascribe functional domains in this segment of the protein we constructed eight different 20-amino-acid deletion derivatives of this factor. Figure 1B shows the results of overexpressing these deletion mutants in the *prp17* null yeast strain SJ136. As

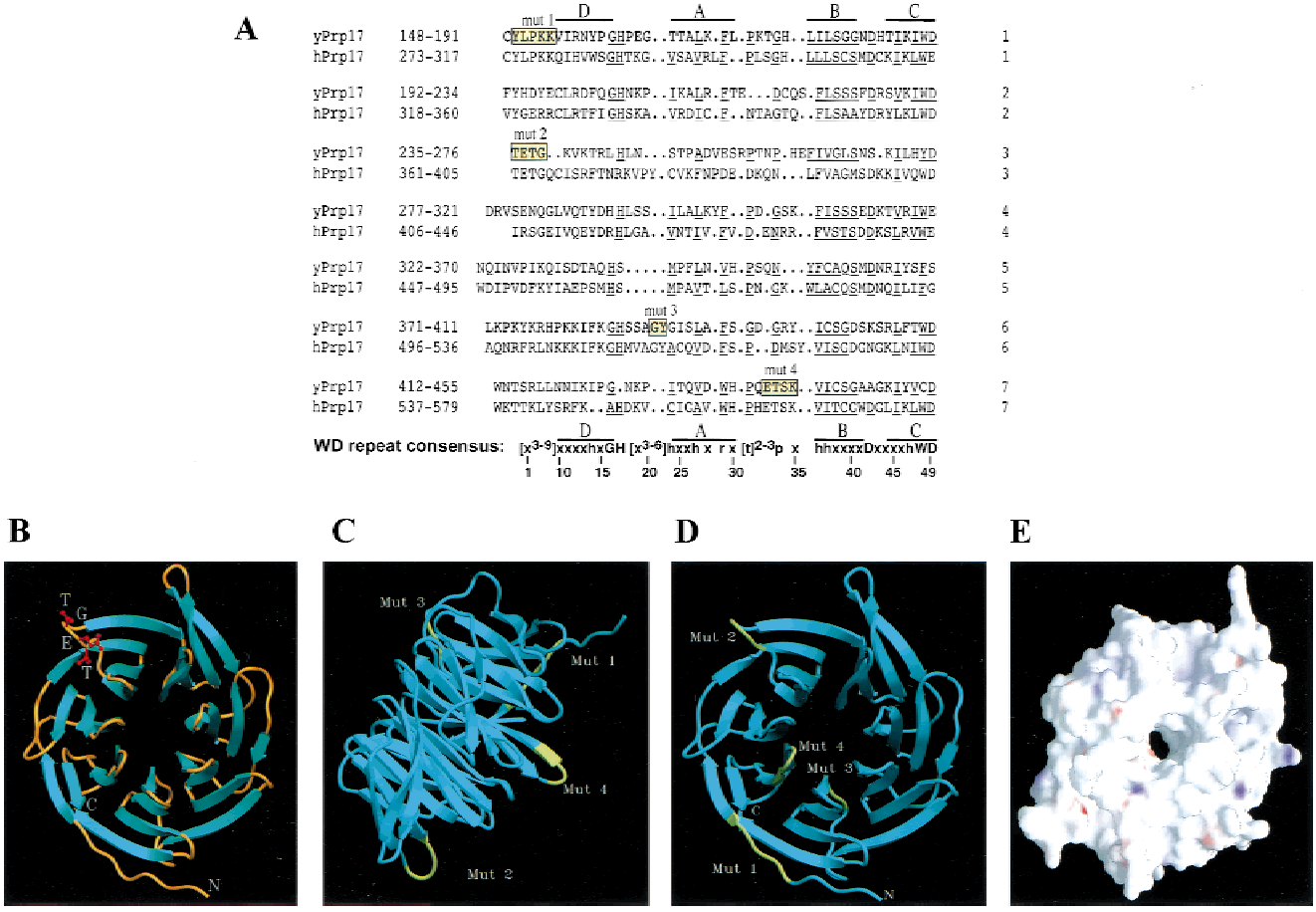

FIGURE 2. Comparative modeling of the Prp17p WD domain. **A**: Alignment of WD repeats of yPrp17p and hPrp17. Amino acid sequences were aligned using PILEUP (Genetics Computer Group), and a period was introduced for alignment between conserved residues. The underlined amino acids are highly conserved in the WD repeat. The WD-repeat consensus according to Neer and Smith (1996) is shown on the bottom, where each position is assigned a number, and x is a nonconserved position, h is a hydrophobic position, r is a conserved aromatic, p is a conserved polar position, and t is a tight turn containing glycine, proline, aspartic acid, or asparagine. The position of the four β strands are indicated as A, B, C, and D. The four mutations generated in yPrp17p are boxed in yellow and labeled. **B**: Overall fold of the model of the WD region of yPRP17p. The β-sheet regions are shown in light green and the loop regions in brown. The side chains of three of the residues, Thr-Glu-Thr, in the Mut2 region are shown in red. N and C refer to the amino and carboxy ends of the domain. This figure and Figure 3C were generated using SETOR (Evans, 1993). **C**: Overall fold of the modeled structure in a side view different from that in panel B. The sites of the mutations (Mut1 to Mut4) are shown in yellow. **D**: The regions of the protein mutated in Mut1 to Mut4 shown in yellow in the propeller fold. **E**: The electrostatic potential surface of the model of yPrp17p as seen from the broader face of the fold; Mut1, Mut2, and Mut4 were constructed on this face. The acidic and basic patches are shown in red and blue, respectively, and white refers to a neutral charge. The image was produced using the program GRASP (Nicholls et al., 1991).

previously reported, the knockout strain, when transformed with vector alone (pG1), has a severe temperature-sensitive phenotype, as is known for the *prp17* null strains (Jones et al., 1995; Seshadri et al., 1996; Lindsey & Garcia-Blanco, 1998). It grew poorly at room temperature and 30 °C, and did not grow at 34 °C or 37 °C (Figs. 1B,C and 3B). The growth defect was rescued by wild-type HAyPrp17 (Figs. 1B,C and 3B). Five of the eight deletions were still fully functional (Fig. 1B). However, deleting amino acids 102–121 or 122–141 did not allow yPrp17p to fully rescue the temperature-sensitive phenotype (Fig. 1B). Examination of the sequence conservation within these regions revealed very high homology (65% identity) between the yeast and human proteins between amino acids 122–141. This degree of conservation, along with the results from deleting these amino acids, suggests that it may be a region important for Prp17 function. Significantly, one of the temperature-sensitive *prp17* missense mutants, *prp17-1*, lies in this segment (Seshadri et al., 1996). In the region amino acids 102–121, only 20% identity exists between the yeast and human proteins, but our results suggest that it constitutes an important domain. Deleting amino acids 142–161 did not rescue the null phenotype at all (Fig. 1B), but as discussed later, this deletion includes part of the first WD domain and may result in improper folding of the domain.

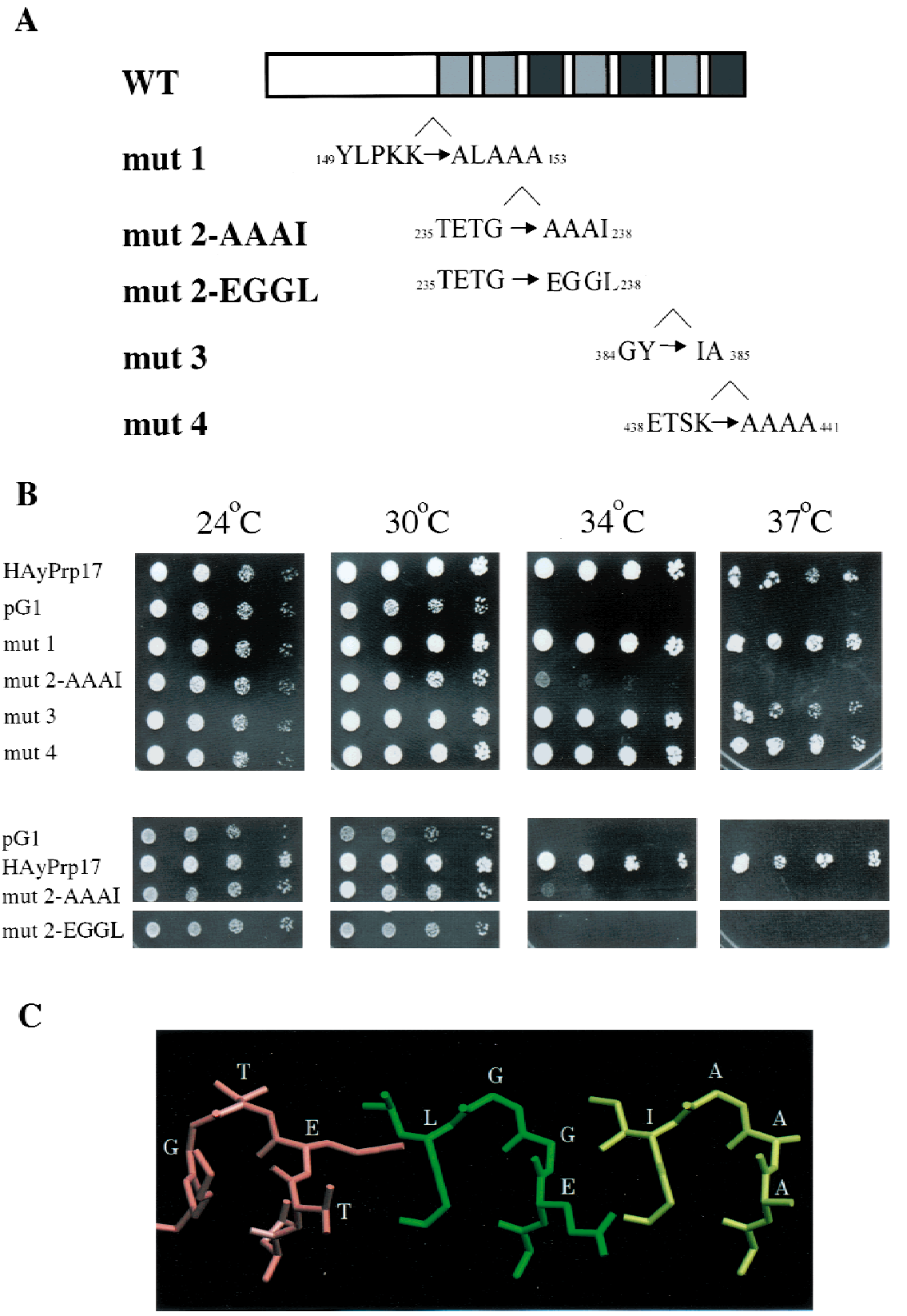

FIGURE 3. Mutational analysis of the WD domain of yPrp17p. **A**: Five mutations (Mut1, Mut2 AAAI, Mut2 EGGL, Mut3, and Mut4) were made in the WD domain of yPrp17p. **B**: The Δ*prp17* yeast strain was transformed with the wild-type HAyPRP17, the pG1 vector alone, or with pG1 containing the mutated PRP17 sequences. Fivefold serial dilutions were made of the yeast, which were then grown on medium lacking tryptophan at 25 °C, 30 °C, 34 °C, or 37 °C. **C**: The close-up of the main chain and side chains of amino acid residues in the loop targeted for mutation in Mut2. Left panel: wild-type protein with the sequence TETG; center panel: Mut2 with the sequence EGGL; right panel: Mut2 with the sequence AAAI.

We also made larger deletions within the segment encoded by the N-terminal 158 amino acids to determine the minimum region required for function. Deletion of up to 110 amino acids from the N-terminus resulted in a protein that fully rescued the temperature-sensitive phenotype of the knockout yeast strain, whereas deletions of amino acids 1–120, 1–130, and 1–140 were only partially functional (Fig. 1C). These findings are significant because they show that the first 110 amino acids of yPrp17p were not essential for its function. Under these experimental conditions, only 40 amino acids were required N-terminal to the WD domain for a completely functional protein, and deletion of the whole N-terminus up to the WD domain resulted in a partially functional protein. Therefore, these results suggest that the WD domain contains a significant functional region of yPrp17p.

Comparative modeling of the Prp17p WD domain

The crystal structure of the prototypical member of the WD-repeat family, Gβ, has been solved complexed with the γ subunit (Sondek et al., 1996) or with both α and γ subunits (Wall et al., 1995; Lambright et al., 1996). The Gβ subunit folds into a highly symmetrical seven-blade β propeller. Each propeller blade consists of a small four-stranded twisted β sheet. The N-terminal amphipathic α helix interacts closely with the Gγ subunit, which is required for the correct folding and function of the Gβ subunit. It has been predicted that all the WD-repeat proteins will form the same propeller fold because of the conservation of amino acid residues involved in important structural interactions (Neer & Smith, 1996). For example, the highly conserved aspartic acid (D_{42}) between strands B and C is involved in the formation of an inter-blade and intra-blade hydrogen-bonded tetrad with histidine (H_{17}) in the GH motif, a serine or threonine at position 38 of the B strand, and tryptophan (W_{48}) (see Fig. 2A for numbering). The propeller fold can be quite forgiving, however, as propellers can form without any of these amino acids (Neer & Smith, 1996). Another important structural interaction is provided by the aromatic residues near the end of in the A strand (position 29) and the C-terminal tryptophan (W_{48}). The aromatic rings form a hydrophobic surface on the blades, stabilizing the connections between neighboring propeller blades.

The alignment of the C-terminal WD domains of yPrp17p and hPrp17 is shown in Figure 2A. The residues that are conserved among the WD-repeat family are underlined, and the four β strands of each repeat are indicated (A, B, C, and D). Before attempting a mutational analysis of the WD domain of yPrp17p, we generated a three-dimensional model of the WD repeat region of yPrp17p on the basis of the known structure of the G protein β subunit determined as a heterotrimeric G$\alpha\beta\gamma$ complex (Wall et al., 1995; Lambright et al., 1996; Sondek et al., 1996). Because of the low similarity between the amino acid sequences of the WD region of yPrp17p and Gβ, we performed the alignment after taking into consideration the three-dimensional structural features of Gβ (such as solvent accessibility and secondary structure) and the relationships at individual residue positions (such as hydrogen-bonding patterns). Compatibility of a residue in yPrp17p with the structural environment of the candidate equivalent residue in Gβ was verified. These considerations were necessary because sequence identity between yPrp17 and Gβ is only 15.3%. Additionally, alignment of residues in Gβ with the human Prp17 protein, which shows a slightly higher sequence identity with Gβ (21%), was also taken into consideration (data not shown). The sequence similarity (which considers the occurrence of nonidentical, but similar residues in the aligned positions) between yPrp17p and Gβ is about 56%.

The sequence of yPrp17p could be comfortably accommodated in the Gβ propeller fold (Fig. 2B). Each of the seven propeller blades is composed of four antiparallel β strands with the A strand innermost in the propeller, followed outwardly by B, C, and D. The WD repeat in the primary sequence corresponds to the outer strand (D) of one β blade and the first three inner strands (A, B, and C) of the next. Figure 2C depicts a side view of the propeller structure with a top narrow surface and a bottom broad surface that displays the loops between β strands. The length of the loops located between the β strands of the propeller is variable. The shortest loops, D–A and B–C, are facing the narrow face of the propeller, and the longer loops, A–B and C–D, face the other side. The amino acids in these loops are not conserved among the WD-repeat proteins and likely contribute specific protein–protein interaction surfaces. Almost all the β-strand regions of Gβ are conserved with respect to yPrp17p. The N-terminal helix of Gβ is not modeled in yPrp17p as the sequence similarity is too low, although a helix conformation for this region of yPrp17p cannot be precluded.

Mutational analysis of the WD-repeat domain of yPrp17p

Both the crystal structure of Gβ and mutational analyses of other WD-repeat proteins suggest that the residues in the loop regions between the β sheets are primarily responsible for protein–protein interactions (Wall et al., 1995; Lambright et al., 1996; Sondek et al., 1996; Komachi & Johnson, 1997; Ford et al., 1998). Therefore, we decided to identify critical residues in the loop regions of yPrp17p. We chose not to simply make deletions in the WD domain for fear of disrupting the overall structure of the protein. Instead, we chose to mutate four different loop regions that contain identical

amino acid residues in the yeast and human proteins. The latter rationale is supported by the finding that although the full-length human protein bears only 36% overall identity to the yeast Prp17, it can partially rescue the null yeast strain (Ben Yehuda et al., 1998; Lindsey & Garcia-Blanco, 1998). The residues targeted for mutational analysis are boxed in Figure 2A, and the locations within the predicted three-dimensional structure are shown in Figure 2C,D. Figure 3A details the mutations, and Figure 3B shows the results of overexpressing the mutants in the *prp17* null yeast strain. Mutations 1, 3, and 4 all behaved as wild type; however, mutation 2 could not rescue the temperature-sensitive phenotype (Fig. 3B). Therefore, the four amino acids, $_{235}$TETG$_{238}$, are important for the function of yPrp17p. Because these amino acids are predicted to reside on the surface of yPrp17p (Fig. 2C,D), they may be involved in mediating macromolecular interactions. The model of the wild-type protein suggests that these amino acids are located between two β strands and form a solvent-exposed loop structure (Fig. 3C, left). In fact, modeling of this region required a deletion in the alignment with respect to Gβ. Analysis of this region suggests that the T_{235} residue is buried with its polar group, forming a hydrogen bond with the buried side chain of an Arg residue. The nonpolar part of the T_{235} side chain is in a hydrophobic interaction with a few nearby nonpolar residues. The three residues following T_{235} in this region, E-T-G_{238}, are all highly solvent exposed. The side chains of the second and third residues (E_{236} and T_{237}) are positioned in such a way that they do not interact with any residue within the WD part of yPrp17p. Hence it seems that replacement of these two residues by other residues may not have a profound effect on the structure. The fourth residue in the sequence, G_{238}, adopts a left-handed α-helical conformation (with ϕ,ψ values of 65°, 35°) that is generally unfavorable for residues larger than Gly due to short nonbonded distances involving the side chain and the main chain.

To investigate the specificity required of these residues, we also substituted these four amino acids with the equivalent residues (EGGL) found in the WD domain splicing protein Prp4p. This mutated Prp17 protein (TETG $\rightarrow$ EGGL) was also unable to rescue the temperature-sensitive phenotype of the null yeast strain (Fig. 3B). However, individual alanine substitutions at position 236 or position 237 performed as wild type in this assay (data not shown), corroborating the structure-based predictions for these two residues. None of the mutant proteins had dominant negative phenotype in the wild-type strain (data not shown).

We have generated models of two of the mutants that correspond to the Mut2 region involving the sequence changes TETG $\rightarrow$ AAAI and TETG $\rightarrow$ EGGL. The models provide further evidence that this region is important for the function of yPrp17p. Figure 3C (center and right) shows the close-up of this loop in these mutants. Replacement of T_{235}, which is buried in the wild-type protein, by A in Mut2 AAAI results in loss of the interaction with Arg as well as producing a void space (due to a shorter side chain replacing a longer side chain). Hence, repacking of the residues in the vicinity is likely to take place to fill the otherwise void volume (Fig. 3C, right). In Mut2 EGGL, Glu replaces T_{235}. This replacement requires accommodation of a longer side chain (Glu), which could result in conformational changes in the vicinity (Fig. 3C, center). Hence, in both of these mutants, there is a likely alteration in the structure and packing of the loop compared to the wild type. Although replacement of G_{238}, which is in a left-handed α-helical conformation, with nonglycyl residues is generally unfavorable, replacement of such a Gly with Ile (as in Mut2 AAAI) and Leu (as in Mut2 EGGL) is drastic. Both Ile and Leu are well known to be highly unfavorable for the left-handed, α-helical conformations. These replacements at position 235 and 238 are likely to significantly alter the loop structures in these mutants. We have also examined the structural consequences of mutations in the residues $_{438}$ESTK$_{441}$ that we have termed Mut4. Most of these residues are also surface exposed in the model (Fig. 2C,D), and this region corresponds to an exposed β strand immediately following a β hairpin loop. Interestingly, this region has a bulge disrupting the hydrogen-bonding pattern with the other strand in the β hairpin. In Mut4 all four of these residues are replaced by alanine. Presence of two hydrophobic residues (Val 432 and Trp 434) in the other β strand could influence the side chain of most of these alanines so that a small hydrophobic environment results. Thus the conformation of the main chain in Mut4 is not expected to be significantly altered, and the series of alanines in this mutant are expected to be stabilized by a subtle alteration in the side chain conformation, resulting in a small hydrophobic environment (data not shown). Three of the mutations generated (Mut1, Mut2, and Mut4) occur on the more open face of the β propeller fold (Fig. 2C,D). An electrostatic representation of this region was obtained using the GRASP program (Fig. 2E; Nicholls et al., 1991). This face of the propeller structure is largely uncharged, except for a few small regions of positive and negative charges. Hence, any macromolecular interactions involving this face of Prp17p may not be mediated by charge complementarity.

We have also examined the defects in pre-mRNA splicing in the strains with *prp17 mut2* alleles and also with *prp17 Δ142–161*. The results from these analyses correlate the viability data with biochemical defects. Splicing of transcripts from the chromosomal *ACT1* gene was assayed by RT-PCR with primers designed to detect pre-mRNA and the lariat intermediate. Wild-type strains grown at 23 °C or 37 °C do not accumulate precursors or intermediates of splicing, in contrast to strains

with a null allele of *prp17* that accumulate lariat intermediate and pre-mRNA (Fig. 4A). Both of the *mut2* alleles, *TETG-AAAI* and *TETG-EGGL*, are significantly defective for the second step; they accumulate actin lariat intermediates (Fig. 4A). A similar defect is also seen in the *prp17 Δ142–161* allele. These data are in contrast to the weak splicing defect observed in *mut4*, which has phenotypically wild-type growth characteristics (Figs. 4 and 3B). Therefore, we infer from the results of mutating the TETG loop, that this domain of yPrp17p is required for the second step of the splicing reaction.

Mutated yPrp17p protein levels are stable as determined by western analysis

To analyze the inability of some of the mutated yPrp17p proteins to rescue the temperature-sensitive phenotype of the knockout yeast strain, we verified the expression levels of the mutated proteins. Because all of the proteins contained a hemagglutinin (HA) epitope tag at the N-terminus, we tested extracts from each transformed yeast strain by western analyses using anti-HA antibodies (Fig. 5). As a control, the levels of TATA binding protein (TBP) were also examined, because it is a general transcription factor and its protein levels should remain constant, and because its gene does not contain an intron. The mutant protein levels varied significantly when compared to the levels of the wild-type HAyPrp17 expressed from the same plasmid vector. Some mutant proteins were expressed at levels significantly higher than HAyPrp17 (e.g., Δ42–61), and others had significantly lower levels of protein (e.g., Mut2, Mut4, Δ22–41, and Δ142–161) (Fig. 5). Given the overexpression of all these proteins compared to Prp17p levels in wild-type cells (HAyPrp17 protein levels were roughly 50 times higher than endogenous yPrp17p; data not shown), these findings are not unexpected. The lower protein levels in Δ142–161, which deletes the D β strand of the first WD repeat, is likely due to disruption of global structure and therefore stability. Notably, this protein also appears to migrate aberrantly on SDS-PAGE, further suggesting that it may be folding differently than the other proteins. Because some of the mutations that had low protein levels (e.g., Mut4 and Δ22–41) were still capable of completely rescuing the temperature-sensitive phenotype of the null yeast strain (Figs. 1B and 3B), we conclude that the loss of function seen with Mut2 is not related to the level of protein.

Subcellular localization of yPrp17p and the mutated proteins shows a nuclear localization signal in the N-terminal domain

We used immunofluorescence to determine the localization of the epitope-tagged proteins. Because of its role in pre-mRNA splicing, the reports on nuclear localization of the human and yeast proteins is not surprising (Boger-Nadjar et al., 1998; Lindsey & Garcia-

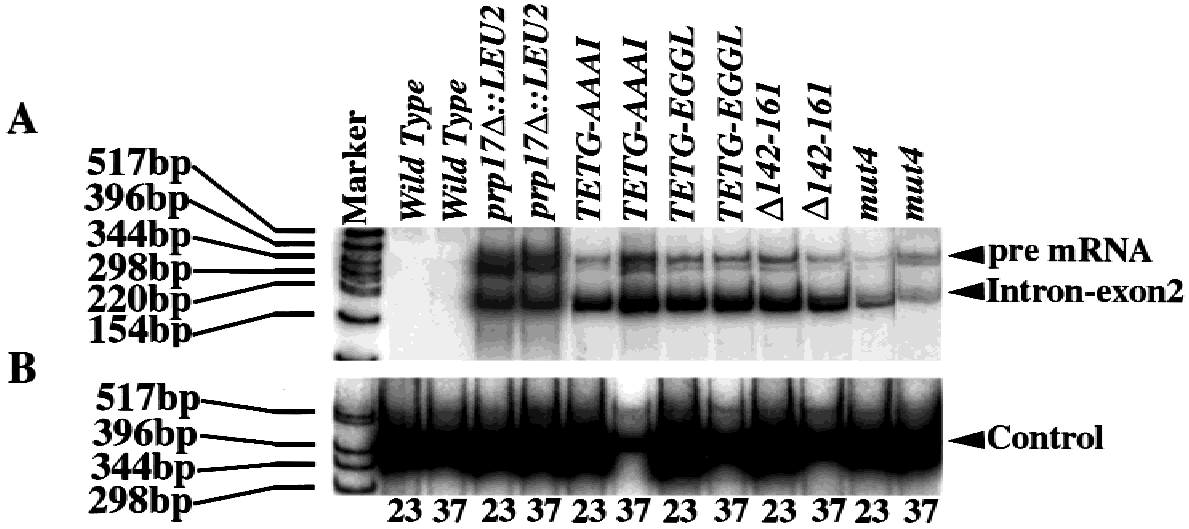

FIGURE 4. Splicing defects in *prp17* mutant alleles. **A**: RT-PCR analysis for splicing of ACT1 transcripts. cDNA was generated using a primer 5′ of the *ACT1* branch point; and PCR was done with the same primer together with a primer at the 5′ end of Exon 1 and another primer in the intron downstream to the 5′ splice site. Total RNA (15 μg) used was from each of the six different strains denoted above the lanes (*Wild type, prp17Δ::LEU2*, *prp17Δ::LEU2+pG1mut2(AAAI)*, *prp17Δ::LEU2+pG1mut2(EGGL)*, *prp17Δ::LEU2+pG1Δ142–161*, and *prp17Δ::LEU2+mut4*) and was prepared from cells grown at both permissive and nonpermissive temperatures, as indicated at bottom. The PCR products from the pre-mRNA and Lariat intermediate are indicated. End-labeled pBR322 digested with *Hin*fI was used as molecular weight marker. **B**: RT-PCR analysis of *PRP24* transcripts, from a nonintron-containing gene, as control. Total RNAs prepared from the strains denoted in **A** were used for RT-PCR with primers specific to a segment of *PRP24* mRNA.

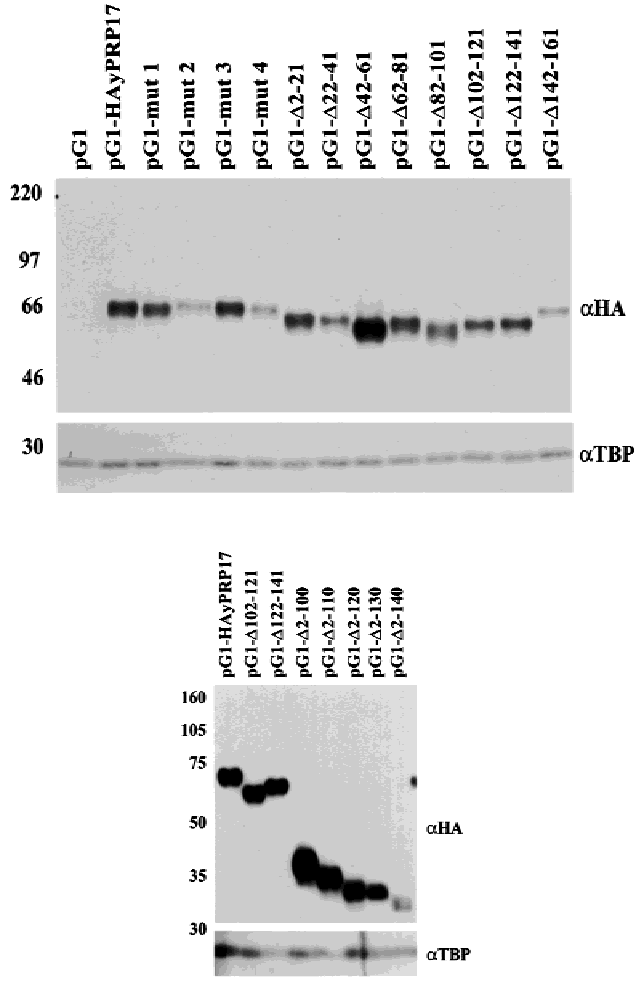

FIGURE 5. Western analysis to determine protein levels. The Δprp17 yeast with the specified plasmid were grown in selective media until mid-log phase, transferred to 37 °C for 2 h, and then lysed in cracking buffer. Equal cell numbers were loaded onto SDS-PAGE and then transferred for western analysis. The blots were probed with antibodies against the HA epitope tag, and then stripped and reprobed with a TBP antibody as a loading control.

Blanco, 1998). In fact, we observed uniform nuclear staining of HAyPrp17 (Fig. 6). In addition, all mutant proteins showed exclusive nuclear localization except for Δ42–61 and the N-terminal deletions Δ2–100 through Δ2–140 (Fig. 6 and data not shown). Thus, whenever amino acids 42–61 were absent, the protein accumulated in the cytoplasm. This basic stretch of amino acids (NNIHKRKSHFTKSELKRRRK) was previously predicted to be the nuclear localization signal (NLS) for this protein (Vaisman et al., 1995). Our data adds functional support that this is indeed the NLS. Significantly, the Δ42–61 protein, as well as Δ2–100 and Δ2–110, were still able to rescue the temperature-sensitive phenotype when overexpressed in the knockout strain. This suggests that a minor, but functionally sufficient, level of yPrp17p accumulates in the nucleus in this strain.

Genetic interactions among *prp17* and U5 snRNA mutations

U5 snRNA is essential in yeast and is required for mammalian in vitro splicing. Genetic and crosslinking studies have implicated the invariant loop I sequence of U5 snRNA in an interaction with exon sequences adjacent to the splice sites (Frank et al., 1992; O'Keefe et al., 1996; Seshadri et al., 1996; Xu et al., 1998). Detailed analyses of loop I sequences revealed that their interaction with exonic sequences are not necessary for the first catalytic step but are critical for the second step of splicing in yeast (O'Keefe & Newman, 1998). In addition, a number of U5-associated protein factors are required at this step. One likely function for these factors is in maintaining an active conformation of the catalytic spliceosome. Consistent with these findings, are reports that alleles of *PRP17* interact genetically with loop I of U5 snRNA. *prp17-3/slu4-1* was isolated as a temperature-sensitive mutation that was synthetically lethal with a specific U98A mutation in loop I of U5 snRNA (Frank et al., 1992). Later it was shown that the *prp17-3* allele was allele specific in its interaction with U5 snRNA and that three other alleles, *prp17-1*, *prp17-2*, and *prp17Gβ3–9*, did not show this interaction (Seshadri et al., 1996; Table 1, bottom). The mutation in *prp17-3* lies in the N-terminal domain that is not conserved between the yeast and the human proteins. More recently, another temperature-sensitive allele of *PRP17*, *prp17-100/slt15*, was identified in a screen for synthetic lethality with U2 snRNA mutations (Xu et al., 1998). The mutation in this allele has not been mapped, but it was lethal in combination with both the U98A and the UU97,99CC U5 snRNA mutations (Xu et al., 1998; Table 1, bottom).

We wanted to examine whether the mutations generated here, particularly in loop regions of the predicted β propeller of Prp17p, interact with any of the three previously described U5 snRNA loop I mutations (Fig. 7B). The strategy adopted was to transform the different plasmid-borne *prp17* mutations into a haploid strain that bears chromosomal null alleles for both the *PRP17* gene and the *SNR7* gene that encodes U5 snRNA (Fig. 7A). This haploid strain was kept viable by expressing a plasmid-borne wild-type *SNR7* gene under the control of the *GAL1* promoter. After transformation of the mutant *prp17*-bearing plasmids, the strain was again transformed with one of three plasmids that contained mutant *SNR7* alleles (*U98A, U98C*, or *UU97,99CC*) under the control of their endogenous promoter. Finally these transformants were examined for growth on glucose-containing plates, conditions which repress the transcription of the wild-type *SNR7* gene. These experiments test the interaction between *prp17* alleles and the mutant U5 snRNA (Fig. 7C and Table 1). Out of all of the alleles analyzed, only three alleles of *prp17* showed an allele-specific interaction

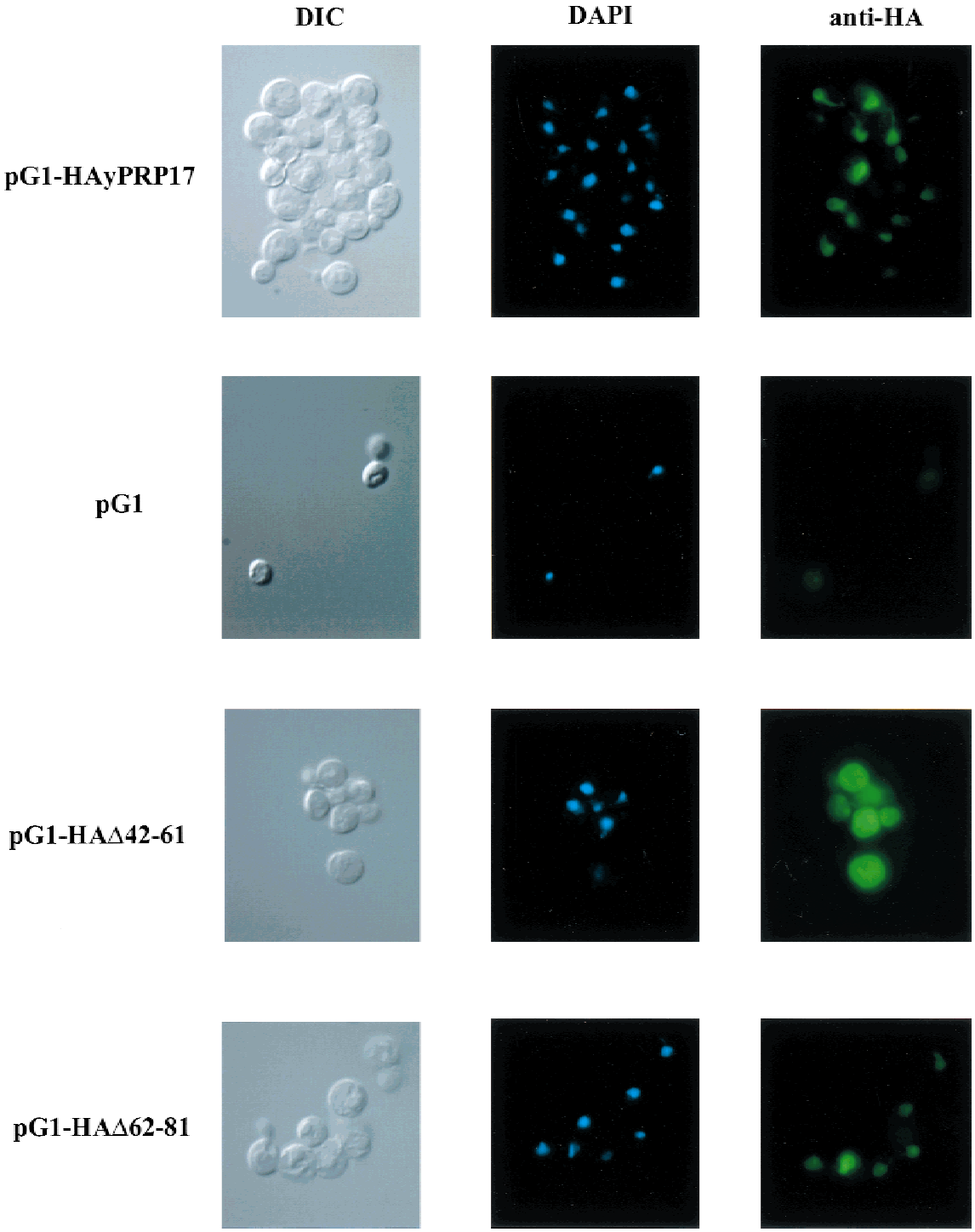

FIGURE 6. Localization of yPrp17p and the mutated proteins. Immunofluorescence was performed with a mouse monoclonal antibody against the N-terminal HA tag of the proteins and a secondary anti-mouse IgG coupled to fluorescein (right column). DAPI, which stains DNA, was used to visualize the nuclei (middle column). Differential interference contrast (DIC) images of the cells are also shown (left column). All the mutations have been examined, and a few representative examples are shown here. The wild-type protein, pG1-HAyPrp17 (top row) and Δ62–81 (bottom row) have strong nuclear staining. Δ 42–61 (third row from the top) has cytoplasmic localization, and therefore the deleted amino acids probably contain the NLS. Yeast expressing the pG1 vector alone are shown as a control (second row).

with a particular mutation in U5 snRNA (*U98A*) (Table 1 and Fig. 7C). These were *TETG* → *EGGL, TETG* → *AAAI* and Δ*142–161*. These data suggest allele-specific interactions between *PRP17* ($_{235}$TETG$_{238}$) and U5 snRNA. These amino acids may, therefore, be involved in mediating a direct or indirect interaction with U5 snRNA. These data, together with the second-step splicing defect observed in these *prp17* alleles, suggest a

TABLE 1. Summary of synthetic lethal interactions between *prp17* mutations and U5 snRNA loop I mutations; viability of haploid *prp17snr7* double mutants; grown on YP glucose.

	snr7 allele		
prp17 allele	U98A	*U98C*	*UU97,99CC*
prp17::LEU2	−	+	+
Δ2–21	+	+	+
Δ22–41	+	+	+
Δ42–61	+	+	+
Δ62–81	+	+	+
Δ82–101	+	+	+
Δ122–141	+	+	+
Δ142–161	−	+	+
mut2 (amino acids 235–238)			
TETG → AAAI	−	+	+
TETG → EGGL	−	+	+
TETG → TEAG	+	+	+
TETG → TATG	+	+	+
mut4 (amino acids 438–442)			
ETSKV → AAAAP	+	+	+
prp17-1(G127A)[a]	+	+	+
prp17-2(R58G)[a]	+	+	+
prp17-3(S54L)/slu4-1[a,b]	−	+	+
prp17-100/slt15 (ND)[c]	−	ND	−

Symbols: +: the double mutant is viable and without additive defect; −: the double mutant is lethal (i.e., it has synthetic lethality); ND: not determined.

[a]See Seshadri et al., 1996.

[b]See Frank et al., 1992.

[c]See Xu et al., 1998.

functional overlap with U5 snRNA during the second step of splicing. These analyses again point to an important role for this loop in the WD domain of Prp17p.

DISCUSSION

yPrp17p has been shown to be required for efficient completion of the second step of pre-mRNA splicing (Vijayraghavan et al., 1989; Frank & Guthrie, 1992; Frank et al., 1992; Jones et al., 1995; Lindsey & Garcia-Blanco, 1998). However, the exact function of yPrp17p during pre-mRNA splicing and its interacting partners are not yet fully understood. In this study, we have conducted a structure–function analysis of yPrp17p to identify amino acids that are required for its function. The C-terminal 300 amino acids are highly conserved between yPrp17p and hPrp17 (40% identity) and contain seven WD repeats, placing these proteins in the WD-repeat superfamily. Knowledge of the three-dimensional structure of one WD-repeat protein, Gβ, has allowed us to model the structure of yPrp17p. Gβ folds into a circular propeller structure with seven blades, each made up of four β strands (Wall et al., 1995; Lambright et al., 1996; Sondek et al., 1996). Not surprisingly, our modeling of the evolutionary highly conserved C-terminal two-thirds of Prp17p shows that it, too, adopts a β-propeller structure with the classical seven-fold symmetry. A typical WD repeat motif is characterized by GH and WD doublets that are separated by a characteristic pattern of hydrophobic and hydrophilic residues. Not all the GH and WD sequence motifs are present in yPRP17p; however, it is likely to contain seven structural repeats, as the amino acid sequence could be comfortably accommodated into the fold of Gβ without anomalies such as too many exposed nonpolar residues or too many buried polar residues. Indeed, several proteins that do not contain the characteristic WD repeats and have no amino acid sequence similarity to Gβ have been observed to have a seven-fold, symmetric β-propeller fold (Murzin, 1992). For example, the crystal structure of the clathrin heavy chain shows a seven-bladed β propeller closely resembling Gβ, but with no sequence similarity to WD proteins (ter Haar et al., 1998). Murzin (1992) also showed that no strong sequence constraints are necessary for the proper β-sheet twisting and packing required for a seven-fold symmetric structure.

The β-propeller structure, although relatively flat, displays the interspersed protein sequences as loops on two surfaces of the structure. These loop regions within WD-repeat proteins are variable in length and sequence, thus providing diversity among the family members. The WD-repeat structure has been described as a rigid scaffold onto which the variable loops are oriented (Neer & Smith, 1996). The computer model structure of yPrp17p, along with information about the conserved amino acids, enabled us to select specific residues in the loop regions of yPrp17p to mutate. Our mutational analysis of residues in four loops that are conserved between the human and yeast Prp17 proteins reveals a function for one loop on the broad surface of the propeller. Mutations within this loop region, Mut2 ($_{235}$TETG$_{238}$), abolished the ability of the protein to rescue the null phenotype. Changes of $_{235}$TETG$_{238}$ to either AAAI or EGGL resulted in a nonfunctional protein. Structural analysis of these residues in the predicted model revealed that E_{236} and T_{237} were fully surface exposed, whereas T_{235} was partially buried. Mutations in T_{235} are predicted to drastically alter the loop structure and packing compared to the wild-type protein, and therefore, could explain the nonfunctional nature of these mutant proteins. The requirement for Gly at position 238 is likely due to space constraints, as this residue is predicted to adopt a left-handed conformation permissible only for Gly. Occurrence of Gly in the left-handed, α-helical conformation in the loops of β hairpins is commonly seen in protein structures (Sibanda & Thornton, 1985). Replacement of Gly by nonglycyl residues is likely to result in significant conformational changes in the loop. Our results suggest that this loop may be a possible protein-binding site; however the interaction is likely to be mediated by shape complementarity rather than by charge complementarity. Candidate interacting partners are second-step factors such

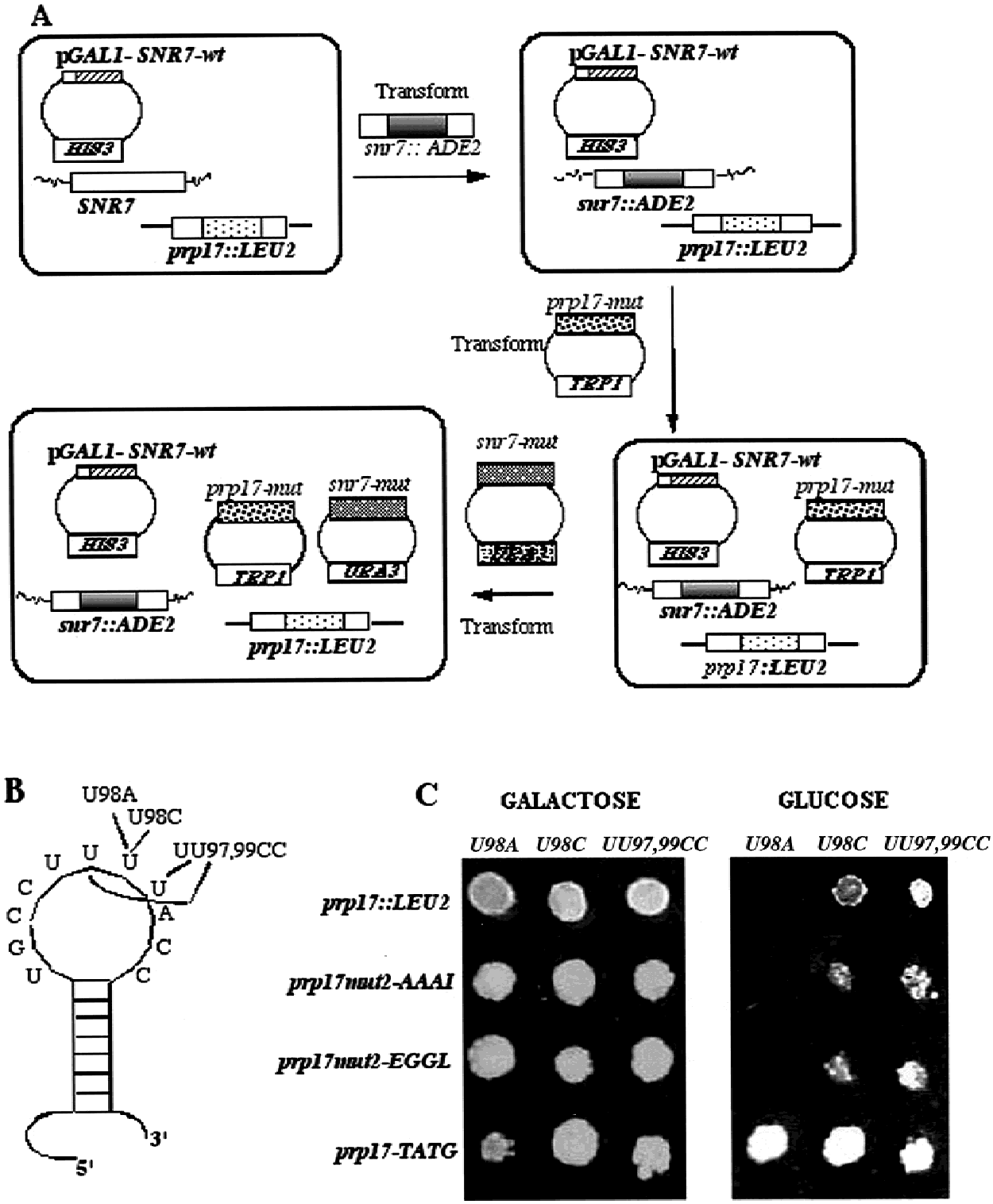

FIGURE 7. Interaction between mutant U5 snRNAs and alleles of *prp17*. **A**: Generation of haploid *prp17::LEU2* with chromosomal disruption of *snr7* and plasmid-borne mutant *prp17* and mutant *snr7*. The haploid strain, YPH274A Δ*prp17::LEU2,* bearing a plasmid-borne copy of pGAL1-*SNR7*, was transformed with a linear fragment of *snr7::ADE2*. The transformants were selected on galactose medium lacking leucine and adenine and then later analyzed for disruption of the chromosomal copy of *SNR7* by Southern analysis. This strain was then transformed with the various mutant alleles of *prp17* and the selected transformants were used to examine interactions with three different mutations in U5 snRNA (*U98A, U98C, UU97,99CC*). This was done by transforming plasmid-borne copies of these mutant U5 snRNAs under the control of their endogenous promoters. These final sets of transformants were analyzed for their ability to grow in glucose-containing medium. **B**: Schematic representation of loop I of U5 snRNA showing the three different mutations (*U98A, U98C, UU97,99CC*) used in the synthetic lethal assay. **C**: Synthetic lethality of mutations in *PRP17* with U5 snRNA mutants. Interactions between the Mut2 *TETG→AAAI*, Mut2 *TETG→EGGL*, Mut2 *TETG→TATG*, or the null *prp17* allele was tested against U98A, U98C, and UU97,99CC. Growth on glucose implies no interaction, whereas lack of growth implies a synthetic lethal interaction.

as Prp8p, Slu7p, and Prp18p, all of which could be tested. Significantly, the amino acids in the loops of many WD proteins, such as Gβ, TUP1, and Prp4p, have been shown to be involved in direct interactions with other proteins (Komachi & Johnson, 1997; Ayadi et al., 1998; Ford et al., 1998). Very recent data suggests that Prp17p may be an auxiliary factor to Prp8p, which is required for precise 3′-splice-site recognition (Ben Yehuda et al., 2000). However, a direct interaction between Prp17p and Prp8p was not detectable in the two-hybrid system (Ben Yehuda et al., 2000).

Two other splicing factors, Prp4p and U5-40kD, contain WD domains. Prp4p is part of the U4/U6 snRNP and interacts with Prp3p through multiple contacts within the loop regions of the WD domain (Ayadi et al., 1998). U5-40kD is a component of U5 snRNP in humans, and no yeast equivalent has been described (Achsel et al., 1998). There is no homology between the loop regions of Prp17p and Prp4p, but, interestingly, there are several regions of similarity between Prp17p and U5-40kD. Significantly, the amino acids following the second WD repeat in U5-40kD are $_{138}$SETG$_{141}$. This is the equivalent position as $_{235}$TETG$_{238}$ in Prp17p. Notable is the fact that the only difference is in the first residue of the loop, that is, Thr *versus* Ser, hinting at a structural role for the −OH groups in these residues. Therefore, we might speculate that these two proteins might interact with the same factor at some point during the splicing reaction. U5-40kD interacts directly with hPrp8, but it is not known which amino acids are involved in this interaction (Achsel et al., 1998). Although a direct interaction between Prp8p and Prp17p has not been reported, we speculate that this loop within the WD domain of Prp17p could be involved. The notion of yPrp17p interacting with a U5 snRNP component is further supported by genetic data that indicates that yPrp17p and U5 snRNA functionally interact (Frank et al., 1992; Seshadri et al., 1996; this study, Table 1).

Disruption of *PRP17* results in temperature sensitivity of the yeast strain (Jones et al., 1995), and our previous studies showed that the human protein, hPrp17, could partially rescue this phenotype (Lindsey & Garcia-Blanco, 1998). Therefore, the amino acids required for function have been conserved from yeast to humans. We also examined whether these mutations interacted genetically with mutations in the loop I of U5 snRNA that is absolutely conserved through evolution. The synthetic lethality of *U98A* U5 snRNA mutation with two mutations in the loop possibly implies functional overlap between Prp17 and U5 in 3′-splice-site definition at the second step. There are no predicted RNA-binding motifs in this factor; also, the charge distribution in the WD motif of the modeled Prp17 does not reveal a likely binding surface for U5 RNA. Therefore this U5 snRNA–Prp17 interaction likely reflects a functional overlap.

The N-terminal 158 amino acids of yPrp17p have an overall sequence identity of only 25% when compared with hPrp17. We have shown here that 110 of these amino acids are not required for yPrp17p to rescue the temperature-sensitive phenotype of the null yeast strain. Our results suggest that amino acids 110–140, which are located immediately before the WD domain and are 52% identical between yeast and human, are important for the function of yPrp17p. It is also interesting to note that one of the original temperature-sensitive alleles of *PRP17* maps to this conserved region outside of the WD domain. Seshadri et al. (1996), showed that the *prp17-1* allele contains a mutation that changes amino acid 127 from glycine to alanine.

We have used immunofluorescence to examine the subcellular localization of all the mutated proteins. HAyPrp17 gives a general nuclear staining (Fig. 6), and this was verified using confocal microscopy (data not shown). Our results are in contrast to a previous report demonstrating that yPrp17p localizes to the nuclear membrane (Boger-Nadjar et al., 1998). We did not observe specific localization of HAyPrp17 to the nuclear membrane, even though we tagged and overexpressed yPrp17p in a manner similar to that of Boger-Nadjar et al. (1998). Results from our localization studies allowed us to determine that amino acids 42–61 are required for yPrp17p to efficiently localize to the nucleus, and, therefore, contain all, or part of, the NLS. Overexpression of proteins lacking these amino acids, however, was still able to rescue the null phenotype. A plausible explanation is that sufficient, but minimal, amounts of the protein accumulate in the nucleus to provide function. Perhaps expression of lower amounts of yPrp17p lacking the NLS may be incapable of rescuing the null phenotype. Lack of efficient nuclear localization would explain the results previously obtained by Seshadri et al. (1996) in which yPrp17p was not functional when amino acids 26–68 were deleted and the protein was expressed from its endogenous promoter after chromosomal replacement. In that report, the localization of the protein was not described, but our results suggest that it would likely be cytoplasmic. It is also important to note that two of the temperature-sensitive alleles, *prp17-2* (R58G) and *prp17-3*/*slu4-1* (S54L), are located within the region that we have determined is important for nuclear localization (Seshadri et al., 1996).

The previous mutational analysis of yPrp17p performed by Seshadri et al. (1996) preceded crystallization of Gβ and the cloning of the human protein, and at the time, yPrp17p was thought to contain only four WD repeats, repeats 1, 2, 4, and 6 (numbering based on seven repeats). Mutation of the highly conserved WD residues of repeats 4 and 6 resulted in a wild-type phenotype (numbering based on seven repeats) (Seshadri et al., 1996). In hindsight, it is not surprising that these mutations resulted in a functional protein, be-

cause the stable β propeller is quite forgiving and can form without these amino acids (Neer & Smith, 1996). However, deletion of an entire WD repeat (repeats 2, 4, or 6) did result in a null phenotype (Seshadri et al., 1996), as does a deletion of WD repeat 7 (data not shown).

Results from our current experiments have refined the prior functional map of yPrp17p and lead us to conclude that an ~40-amino-acid segment immediately preceding the WD domain together with the C-terminal WD domain constitutes the functional Prp17 protein. Furthermore, we have identified four amino acids within the WD domain that are critical for function. These amino acids are predicted to be on the surface of the protein, and analysis of mutations of these residues have allowed us to define a role for Prp17p in the second step of splicing that overlaps with the role of U5 loop I. Our results suggest that they may be involved in an interaction probably with a protein that is important for the second step of splicing.

MATERIALS AND METHODS

Sequence analysis and comparative modeling

The multiple alignment of the WD repeats of yPrp17p, hPrp17, and the bovine β subunit of the heterotrimeric protein G (G β1, Swissprot P04901) was done with the GCG program, Pileup. The suite of three-dimensional modeling programs encoded in COMPOSER (Sutcliffe et al., 1987a, 1987b; Srinivasan & Blundell, 1993; Srinivasan et al., 1996) and incorporated in SYBYL (Tripos Inc., St. Louis, Missouri) was used to generate the three-dimensional model of the WD domain of yPRP17p. The structures of the conserved regions of Gβ have been extrapolated to the equivalent regions of yPRP17p. The variable regions were modeled by identifying a suitable segment, which was identified by searching a data bank of known protein structures. A template-matching approach (Topham et al., 1993) to rank the candidate loops was also used. The best ranking loop with no short contacts with the rest of the protein was fit using the ring-closure procedure of F. Eisenmenger (unpubl. results). Side chains were modeled either by extrapolating from the equivalent positions in the basis structure, where appropriate, or by using rules derived from the analysis of known protein structures (Sutcliffe et al., 1987b).

The replacement of the amino acid side chains was performed using the rules coded in the COMPOSER program, which uses the knowledge base of rotamer libraries. The mutant structures were energy minimized as described here. The COMPOSER-generated models were energy minimized in SYBYL using the AMBER force-field (Weiner et al., 1984). Energy minimization cycles were performed until all short contacts and inconsistencies in the geometry were rectified. The stereochemical quality of the final model was ensured by the program PROCHECK (Laskowski et al., 1993). The model was analyzed using interactive graphics in SYBYL and SETOR (Evans, 1993).

Plasmid construction and mutagenesis

A 0.7-kb DNA fragment containing part of the coding region of *yPRP17* was PCR amplified from the previously described plasmid, pG1-yPRP17 (Lindsey & Garcia-Blanco, 1998). The forward primer y17FHAtag (Table 2) introduces an influenza virus HA epitope tag (Kolodziej & Young, 1991) at the N-terminus and creates two restriction sites (*Bam*HI and *Nco*I), which were used for subcloning. The reverse primer y17R25 contained the unique restriction site, *Sac*I, located at nt 650 of the *yPRP17* coding sequence. The *Bam*HI/*Sac*I PCR product was inserted between the same sites of pG1-yPRP17, and the resulting plasmid was named pG1-HAyPRP17.

Subcloning PCR-amplified fragments into the pG1-HAyPRP17 vector created all of the yPRP17 deletions and mutations. PCR products were sequenced to verify that additional mutations were not unintentionally generated. The *yPRP17* mutations and deletions were generated using the "megaprimer PCR" method in which two rounds of PCR are performed (Tao & Lee, 1994). Mut1 was generated using yFmut1 forward primer and y17R25 reverse primer in the first PCR reaction. y17F24 forward primer was used in the second reaction with the first PCR product as a megaprimer. The *Nco*I/*Sac*I-digested product was inserted into the corresponding sites of pG1-HAyPRP17. Similarly, Mut2 was made using yFmut2 forward primer and y17R22 reverse primer in the first reaction and y17F24 forward primer and the prior PCR products as a megaprimer in the second reaction. The *Nco*I/*Hin*dIII-digested product was inserted into the corresponding sites of pG1-HAyPRP17. Likewise, Mut3 and Mut4 were generated using yFmut3 and yFmut4 forward primers, respectively, and y17R9 reverse primer in the first reaction. Forward primer y17F26 was used in the second reaction, and the *Sac*I/*Sal*I-digested product was inserted into the corresponding sites of pG1-HAyPRP17.

The N-terminal 20-amino-acid deletions were generated with a forward primer designed to anneal to 16–18 nt on each side of the deletion. The primers are listed in Table 2, and the deletions are indicated with (/). The reverse primer in the first reaction was y17R25. The PCR product was used as the reverse primer in the second round of PCR, and y17F24 was the forward primer. The *Nco*I/*Sac*I fragment was then inserted between the same sites of pG1-HAyPRP17. The N-terminal deletions (Δ2–21, Δ2–100, Δ 2–110, Δ 2–120, Δ 2–130, and Δ 2–140) were generated with the appropriate forward primer and with y17R26 reverse primer. The PCR product was then digested with *Nco*I and *Sac*I and subcloned into the corresponding sites of pG1-HAyPRP17.

The *snr7::ADE2* allele was created as follows. The plasmid pUC-7HH was created by cloning the *Hpa*I-*Hin*dIII genomic fragment containing *SNR7* into the *Hin*cII-*Hin*dIII sites of pUC18 (Patterson & Guthrie, 1987). A 2.2-kb *Bgl*II fragment containing the yeast *ADE2* gene (Stotz & Linder, 1990) was inserted into the unique *Hin*cII site in the above plasmid to generate pUC18 *SNR7*::*ADE2*. To achieve chromosomal integration of this allele, the plasmid was restriction digested with *Pvu*II prior to yeast transformation. Integration at the *SNR7* locus was confirmed by Southern analysis of several transformants.

TABLE 2. Primers used in this study.

Name	Direction	Sequence of primer
y17FHAtag	F	5′-GGGGATCCAAAATGTACCCATACGACGTCCCAGACTACGCCCATGGTTTAGTAGACGG-3′ (BamHI, NcoI)
y17R9	R	5′-CCGTCGACTAGTCACATACATATATC-3′ (SalI)
y17R22	R	5′-AGCCAAGCTTATCCCATAACCAGCAG-3′ (HindIII)
y17F24	F	5′-CGCCCATGGTTTAGTAGACGGTTATG-3′ (NcoI)
y17R25	R	5′-CAAAGGAAGAGCTCAAAAAAG-3′ (SacI)
y17F26	F	5′-TTTTGAGCTCTTCCTTTGATAG-3′ (SacI)
yFmut1	F	5′-GT**GC**CTTA**G**CA**GC**A**GC**AGTTATACGTAATTATCC**C**GGG-3′ (SmaI)
yFmut2-AAAI	F	5′-GCGTTAA**G**AT**C**TGGGAT**G**CTG**C**A**G**CT**AT**TAAAGTG-3′ (BglII)
yRmut2-EGGL	F	5′-TTTCACTTTA**AG**A**CCT**C**CTC**ATCCCAAAT-3′
yFmut3	F	5′-TCTGCT**AT**T**GC**TGGGATAAGCTTG-3′ (HindIII)
yFmut4	F	5′-GGCATCCTCAAG**C**A**G**CA**GCGGCGCC**CATTTGCAGCGG-3′ (NarI)
Δ2–21	F	5′-CGCCCATGGTTCTGTTCATGAAAAGAAAAAT-3′ (NcoI)
Δ22–41	F	5′-CTTCGACGAAGGCAAA/AATAATATTCATAAGAGA-3′
Δ42–61	F	5′-CGTATGAACCTTCTTCA/ACTCGCAAAGGAGATG-3′
Δ62–81	F	5′-AAAAAGAAGACGGAAA/GCCAGCGAAACTCAGA-3′
Δ82–101	F	5′-CGATGAAACTTCACAA/CTAGATTCGGAACAGA-3′
Δ102–121	F	5′-GCTGGCTGAGGACAAC/GACTATCAAGGCAGAG-3′
Δ122–141	F	5′-TGGTAAATCAGAAAAG/GAAAGGATATCCTTTCG-3′
Δ142–161	F	5′-TGTTGATCTTCGTGAG/CCAGAAGGAACCACTGC-3′
Δ2–100	F	5′-CCCCATGGGGACAACCTAGATTCGG-3′ (NcoI)
Δ2–110	F	5′-CCCCATGGGGAAGTCTCCCATTTTTATGG-3′ (NcoI)
Δ2–120	F	5′-CCCCATGGGAAGGACTATCAAGGCAGAGG-3′ (NcoI)
Δ2–130	F	5′-CCCCATGGGCCACCAAATGACGTCGATG-3′ (NcoI)
Δ2–140	F	5′-CCCCATGGGGAGGAAAGGATATCCTTTCGG-3′ (NcoI)

The restriction sites are underlined and the deletions are indicated with (/). The nucleotides in bold represent the changes introduced during site-directed mutagenesis.

Yeast strains and genetic methods

Yeast haploid strain SJ136 (Δ *prp17*) [kindly provided by C. Guthrie (Jones et al., 1995)] was transformed with plasmids bearing *prp17* mutations. Growth at various temperatures was tested in selective liquid media (SD-Trp). The yeast were diluted to $OD_{600} = 0.1$, and 2 μL of fivefold serial dilutions were spotted onto selective plates, and growth was scored after three to five days at 25 °C, 30 °C, 34 °C, or 37 °C.

The yeast haploid strain YPH274Δ17 (Jones et al., 1995) was used for generating the *snr7::ADE2* allele by homologous replacement with the cloned *SNR7::ADE2* fragment. Prior to this replacement, the *pGAL1-SNR7* plasmid was transformed into YPH274Δ17. The desired *snr7* disruptant was selected on SD-Leu-His-Ade plates. Subsequently, these yeast were transformed with pG1-*prp17* mutant plasmids and *snr7* mutant plasmids to yield strains where growth on galactose *versus* glucose was assayed to determine interaction between mutant *snr7* and *prp17*.

RT-PCR analysis of actin transcripts

Each of the *prp17* mutants were grown in YPD culture to early to mid-log phase of growth ($A_{600} = 0.5–2.0$) and then shifted to nonpermissive temperature 37 °C for 2 h. Cells were pelleted and frozen. Extraction of total RNA was done by the hot phenol method (Vijayraghavan et al., 1989). First-strand cDNA was made from 5–15 μg total RNA in a 20-μL reaction (cDNA cycle kit, Invitrogen). Fifty-microliter PCR reactions were performed with 5 μL of the RT product, 1 μM each of the primers, 0.1 mM of each dNTP and 10 μCi of α-P^{32} dATP. The primer used for reverse transcription was ACT1 UBP (5′-TATCACTATCACTTATCACG-3′), complementary to sequences 42 bp upstream of the branch point of the actin intron. The cDNAs were amplified with the same primer, ACT1 UBP, and two different 5′ primers. The 5′ primer ACT1 5′SS (5′-CCATCCCATTTAACTGTA-3′) was located 19 bp downstream of the 5′-splice-site junction, and the second 5′ primer was located at the 5′ end of actin

exon 1. The size of the amplified PCR product generated from the pre-mRNA was 298 bp, and that generated from the lariat intermediate was 202 bp. In parallel, as controls, RT reactions on the aliquots of the same RNA sample were done using primers specific for *PRP24* (a nonintron-containing gene). The PCR products were visualized after native PAGE where 50 μL of *ACT1* and 20 μL of *PRP24* PCR reactions were electrophoresed.

Yeast extracts and western analysis

Whole-cell extracts were performed as previously described (Printen & Sprague, 1994). Liquid cultures of the transformed yeast strains were grown at room temperature in selective media to $OD_{600} \sim 0.3$, then shifted to 37 °C for 2 h. Then the OD_{600} was again determined, and the OD unit was calculated as $OD_{600} \times$ volume. Subsequently, protein was extracted as previously described (Printen & Sprague, 1994). For western analysis, the gel was transferred onto an Immobilon affinity membrane in 20% methanol, 192 mM glycine, and 25 mM Tris. Following transfer, the blot was blocked in PBS with 5% nonfat dry milk and 0.1% Tween 20. The HA monoclonal antibody (αHA11 from BAbCO) was diluted 1:1,000 in the same buffer and incubated with the membrane at room temperature for 1 h. This was followed by incubation with a peroxidase-conjugated secondary antibody diluted 1:10,000 for 1 h at room temperature, and then reaction was visualized with ECL reagents from Amersham. For subsequent western analysis with anti-TBP antibodies, the membranes were stripped for 5 min in 0.2 N NaOH, washed with water, and then blocked as before. Then the membrane was incubated with a rabbit polyclonal antibody against human TBP (Upstate Biotechnology, Inc.) diluted 1:1,000.

Immunofluorescence and microscopy

Immunofluorescence was performed with slight modifications of previously described protocols (Pringle et al., 1989; Wang & Guthrie, 1998). Yeast were grown in selective media at room temperature to $OD_{600} \sim 0.15$, then diluted in YPD to $OD_{600} \sim 0.1$ and grown until $OD_{600} \sim 0.2$. The yeast were fixed for 1 h with 4.5% final concentration of formaldehyde. The cells were collected, washed, and treated with β-mercaptoethanol and 20 μg/mL Zymolyase 100T in sorbitol buffer (1.2 M sorbitol, 100 mM potassium phosphate buffer, pH 7.5). After 30 min at 37 °C the cells were washed and resuspended in 1 mL sorbitol buffer. Twenty microliters of cell suspension were allowed to adhere to a 0.1% polyethylenimine pretreated slide for 5 min, then aspirated and air dried. The slide was immersed in cold methanol for 6 min and acetone for 0.5 min, then air dried. The slide was preincubated with PBS containing 1 mg/mL BSA, then stained with primary antibody (1:1,000 dilution of mouse monoclonal α HA11) for 1 h, then washed with PBS, and then stained with the secondary antibody (anti-mouse IgG coupled to fluorescein 5-isothiocyanate. The mounting media contained 1 μg/mL 4′,6-diamidino-2-phenylindole (DAPI) for DNA staining. Images were photographed using an Axioskop (Carl Zeiss, Inc.), and color photographs were processed using PHOTOSHOP software (Adobe Systems, Mountain View, California).

ACKNOWLEDGMENTS

We thank C. Guthrie for providing the SJ136 and YPH274Δ17 yeast strains and *SNR7* plasmids, R. Carstens for reading the manuscript, and members of the Garcia-Blanco laboratory for helpful discussions. This work was supported by a grant from the American Cancer Society to M.A.G.-B. L.A.L.-B. is supported by the Raymond and Beverly Sackler Foundation. M.A.G.-B. is an Established Investigator of the American Heart Association and a scholar of the Raymond and Beverly Sackler Foundation. Funding to U.V. was provided by grants from the Council for Scientific and Industrial Research, Government of India, and Wellcome Trust, United Kingdom. N.S. acknowledges grant support from Wellcome Trust, United Kingdom.

Received February 16, 2000; returned for revision March 15, 2000; revised manuscript received June 14, 2000

REFERENCES

Achsel T, Ahrens K, Brahms H, Teigelkamp S, Lührmann R. 1998. The human U5-220kD protein (hPrp8) forms a stable RNA-free complex with several U5-specific proteins, including an RNA unwindase, a homologue of ribosomal elongation factor EF-2, and a novel WD-40 protein. *Mol Cell Biol 18*:6756–6766.

Ansari A, Schwer B. 1995. SLU7 and a novel activity, SSF1, act during the PRP16-dependent step of yeast pre-mRNA splicing. *EMBO J 14*:4001–4009.

Ayadi L, Callebaut I, Saguez C, Villa T, Mornon JP, Banroques J. 1998. Functional and structural characterization of the prp3 binding domain of the yeast prp4 splicing factor. *J Mol Biol 284*:673–687.

Ben Yehuda S, Dix I, Russell CS, Levy S, Beggs JD, Kupiec M. 1998. Identification and functional analysis of hPRP17, the human homologue of the PRP17/CDC40 yeast gene involved in splicing and cell cycle control. *RNA 4*:1304–1312.

Ben Yehuda S, Russell CS, Dix I, Beggs JD, Kupiec M. 2000. Extensive genetic interactions between *PRP8* and *PRP17/CDC40*, two yeast genes involved in pre-mRNA splicing and cell cycle progression. *Genetics 154*:61–71.

Boger-Nadjar E, Vaisman N, Ben Yehuda S, Kassir Y, Kupiec M. 1998. Efficient initiation of S-phase in yeast requires Cdc40p, a protein involved in pre-mRNA splicing. *Mol Gen Genet 260*:232–241.

Burge CB, Tuschl TH, Sharp PA. 1999. Splicing of precursors to mRNAs by the spliceosome. In: Gesteland RF, Cech T, Atkins JF, eds. *The RNA world.* Cold Spring Harbor, New York: Cold Spring Harbor Laboratory Press. pp 525–560.

Chua K, Reed R. 1999. Human step II splicing factor hSlu7 functions in restructuring the spliceosome between the catalytic steps of splicing. *Genes & Dev 13*:841–850.

Couto JR, Tamm J, Parker R, Guthrie C. 1987. A *trans*-acting suppressor restores splicing of a yeast intron with a branch point mutation. *Genes & Dev 1*:445–455.

Evans SV. 1993. *SETOR*: Hardware lighted three-dimensional solid model representations of macromolecules. *J Mol Graph 11*:134–138.

Ford CE, Skiba NP, Bae H, Daaka Y, Reuveny E, Shekter LR, Rosal R, Weng G, Yang CS, Iyengar R, Miller RJ, Jan LY, Lefkowitz RJ, Hamm HE. 1998. Molecular basis for interactions of G protein betagamma subunits with effectors. *Science 280*:1271–1274.

Frank D, Guthrie C. 1992. An essential splicing factor, SLU7, mediates 3′ splice site choice in yeast. *Genes & Dev 6*:2112–2124.

Frank D, Patterson B, Guthrie C. 1992. Synthetic lethal mutations suggest interactions between U5 small nuclear RNA and four proteins required for the second step of splicing. *Mol Cell Biol 12*:5197–5205.

Horowitz DS, Abelson J. 1993. Stages in the second reaction of pre-mRNA splicing: The final step is ATP independent. *Genes & Dev 7*:320–329.

Horowitz DS, Krainer AR. 1997. A human protein required for the second step of pre-mRNA splicing is functionally related to a yeast splicing factor. *Genes & Dev 11*:139–151.
Jones MH, Frank DN, Guthrie C. 1995. Characterization and functional ordering of Slu7p and Prp17p during the second step of pre-mRNA splicing in yeast. *Proc Natl Acad Sci USA 92*:9687–9691.
Kolodziej PA, Young RA. 1991. Epitope tagging and protein surveillance. *Methods Enzymol 194*:508–519.
Komachi K, Johnson AD. 1997. Residues in the WD repeats of Tup1 required for interaction with alpha2. *Mol Cell Biol 17*:6023–6028.
Lambright DG, Sondek J, Bohm A, Skiba NP, Hamm HE, Sigler PB. 1996. The 2.0 Å crystal structure of a heterotrimeric G protein. *Nature 379*:311–319.
Laskowski RA, MacArthur MW, Moss DS, Thornton JM. 1993. PROCHECK: A program to check the stereochemical quality of protein structures. *J Appl Cryst 26*:283–291.
Lindsey LA, Garcia-Blanco MA. 1998. Functional conservation of the human homolog of the yeast pre-mRNA splicing factor Prp17p. *J Biol Chem 273*:32771–32775.
Murzin AG. 1992. Structural principles for the propeller assembly of β-sheets. The preference of the seven-fold symmetry. *Proteins 14*:191–201.
Neer EJ, Schmidt CJ, Nambudripad R, Smith TF. 1994. The ancient regulatory-protein family of WD-repeat proteins. *Nature 371*:297–300.
Neer EJ, Smith TF. 1996. G protein heterodimers: New structures propel new questions. *Cell 84*:175–178.
Nicholls A, Sharp KA, Honig B. 1991. Protein folding and association: Insights from the interfacial and thermodynamic properties of hydrocarbons. *Proteins 11*:281–296.
O'Keefe RT, Newman AJ. 1998. Functional analysis of U5 snRNA loop 1 in the second catalytic step of yeast pre-mRNA splicing. *EMBO J 17*:565–574.
O'Keefe RT, Norman C, Newman AJ. 1996. The invariant U5 snRNA loop 1 sequence is dispensable for the first catalytic step of pre-mRNA splicing in yeast. *Cell 86*:679–689.
Patterson B, Guthrie C. 1987. An essential yeast snRNA with U5 like domain is required for splicing in vivo. *Cell 49*:613–624.
Pringle JR, Preston RA, Adams AEM, Stearns T, Drubin DG, Haarer BK, Jones EW. 1989. Fluorescence microscopy methods for yeast. *Methods Cell Biol 31*:357–435.
Printen JA, Sprague GF Jr. 1994. Protein–protein interactions in the yeast pheromone response pathway: Ste5p interacts with all members of the MAP kinase cascade. *Genetics 138*:609–619.
Schwer B, Guthrie C. 1991. PRP16 is an RNA-dependent ATPase that interacts transiently with the spliceosome. *Nature 349*:494–499.
Schwer B, Guthrie C. 1992. A conformational rearrangement in the spliceosome is dependent on PRP16 and ATP hydrolysis. *EMBO J 11*:5033–5039.
Schwer B, Gross CH. 1998. Prp22, a DExH box helicase, plays two distinct roles in yeast pre-mRNA splicing. *EMBO J 17*:2086–2094.
Segault V, Will CL, Polycarpou-Schwarz M, Mattaj IW, Branlant C, Lührmann R. 1999. Conserved loop I of U5 small nuclear RNA is dispensable for both catalytic steps of pre-mRNA splicing in HeLa nuclear extracts. *Mol Cell Biol 19*:2782–2790.
Seshadri V, Vaidya VC, Vijayraghavan U. 1996. Genetic studies of the PRP17 gene of *Saccharomyces cerevisiae*: A domain essential for function maps to a nonconserved region of the protein. *Genetics 143*:45–55.
Sibanda BL, Thornton JM. 1985. β-hairpin families in globular proteins. *Nature* 316:170–174.
Sondek J, Bohm A, Lambright DG, Hamm HE, Sigler PB. 1996. Crystal structure of a G protein Gbg dimer at 2.1 Å resolution. *Nature 379*:369–374.
Srinivasan N, Blundell TL. 1993. An evaluation of the performance of an automatic procedure for comparative modeling of protein tertiary structure. *Prot Engng 6*:501–512.
Srinivasan N, Guruprasad K, Blundell TL. 1996. Comparative modeling of proteins. In: Sternberg MJE, ed. *Protein structure prediction: A practical approach*. Oxford: Oxford University Press. pp 111–140.
Stotz A, Linder P. 1990. The *ADE2* gene from *Saccharomyces cerevisiae*: Sequence and new vectors. *Gene 95*:91–98.
Sutcliffe MJ, Haneef I, Carney D, Blundell TL. 1987a. Knowledge-based modeling of homologous proteins. 1. Three-dimensional frameworks derived by simultaneous superposition of multiple structure. *Prot Engng 1*:377–384.
Sutcliffe MJ, Hayes FRF, Blundell TL. 1987b. Knowledge-based modeling of homologous proteins. 2. Rules for the conformations of substituted sidechains. *Prot Engng 1*:385–392.
Tao BY, Lee KC. 1994. Mutagenesis by PCR. In: Griffin HG, Griffin AM, eds. *PCR technology current innovations*. Boca Raton, Florida: CRC Press, Inc. pp 69–83.
Teigelkamp S, Newman AJ, Beggs JD. 1995. Extensive interactions of PRP8 protein with the 5′ and 3′ splice sites during splicing suggest a role in stabilization of exon alignment by U5 snRNA. *EMBO J 14*:2602–2612.
ter Haar E, Masacchio A, Harrison SC, Kirchhausen T. 1998. Atomic structure of clathrin: A β-propeller terminal domain joins an α zigzag linker. *Cell 95*:583–573.
Topham CM, McLeod A, Eisenmenger F, Overington JP, Johnson MS, Blundell TL. 1993. Fragment ranking in modeling of protein structure: Conformationally constrained environmental amino acid substitution tables. *J Mol Biol 229*:104–220.
Umen JG, Guthrie C. 1995a. A novel role for a U5 snRNP protein in 3′ splice site selection. *Genes & Dev 9*:855–868.
Umen JG, Guthrie C. 1995b. Prp16p, Slu7p, and Prp8p interact with the 3′ splice site in two distinct stages during the second catalytic step of pre-mRNA splicing. *RNA 1*:584–597.
Umen JG, Guthrie C. 1995c. The second catalytic step of pre-mRNA splicing. *RNA 1*:869–885.
Vaisman N, Tsouladze A, Robzyk K, Ben Yehuda S, Kupiec M, Kassir Y. 1995. The role of *Saccharomyces cerevisiae* Cdc40p in DNA replication and mitotic spindle formation and/or maintenance. *Mol Gen Genet 247*:123–136.
Vijayraghavan U, Company M, Abelson J. 1989. Isolation and characterization of pre-mRNA splicing mutants of Saccharomyces cerevisiae. *Genes & Dev 3*:1206–1216.
Wall MA, Coleman DE, Lee E, Iniguez-Lluhi JA, Posner BA, Gilman AG, Sprang SR. 1995. The structure of the G protein heterotrimer Gia1b1g2. *Cell 83*:1047–1058.
Wang Y, Guthrie C. 1998. PRP16, a DEAH-box RNA helicase, is recruited to the spliceosome primarily via its nonconserved N-terminal domain. *RNA 4*:1216–1229.
Weiner SJ, Kollman PA, Case DA, Singh UC, Ghio C, Alagona G, Profeta S, Weiner P. 1984. A new force-field for molecular mechanical simulation of nucleic acids and proteins. *J Amer Chem Soc 106*:765–784.
Wyatt JR, Sontheimer EJ, Steitz JA. 1992. Site-specific cross-linking of mammalian U5 snRNP to the 5′ splice site before the first step of pre-mRNA splicing. *Genes & Dev 6*:2542–2553.
Xu D, Field DJ, Tang SJ, Moris A, Bobechko BP, Friesen JD. 1998. Synthetic lethality of yeast slt mutations with U2 small nuclear RNA mutations suggests functional interactions between U2 and U5 snRNPs that are important for both steps of pre-mRNA splicing. *Mol Cell Biol 18*:2055–2066.
Zhang X, Schwer B. 1997. Functional and physical interaction between the yeast splicing factors Slu7 and Prp18. *Nucleic Acids Res 25*:2146–2152.
Zhou Z, Reed R. 1998. Human homologs of yeast prp16 and prp17 reveal conservation of the mechanism for catalytic step II of pre-mRNA splicing. *EMBO J 17*:2095–2106.